Simulating measurements from physical modeling by Kirchhoff diffraction method

Lingping Dong , Zhengsheng Yao, Gary F. Margrave and Eric V. Gallant

ABSTRACT

The Kirchhoff diffraction method is used to model physical measurements. This method is based on the wave theory solution of the acoustic wave equation. The acoustic response due to a boundary surface can be expressed as a convolution integral of the source wavelet with an impulse response characterizing the geometry of the boundary surface. The results indicate that the simulated data matches the measurements.

INTRODUCTION

A physical seismic model is often used to assist with an understanding of real world operations. Since the conditions of the physical experiment, (i.e. the physical model parameters, source impulse, source-receiver geometries), are controlled, it is useful to compare data from physical seismic models to numerical modeling solutions. The numerical modeling that can successfully predict the physical model data can be, in turn, a useful tool for enhancing real data interpretations.

During January 1999, a seismic physical model was created at CREWES for the purpose of investigating the effects on seismic resolution of the waves diffracted from edges. In real seismic data, characteristic signatures produced by diffracting edges may indicate geologic faults and possible associated hydrocarbon traps (Kanasewich & Phadke, 1988). Therefore, they have long been of interest in seismology. Mathematical models to account for diffraction usually have been limited to acoustic effects. The geometrical theory of diffraction (Keller, 1962; Kouyoumjian and Pathak, 1974; Zhang et al., 1990) can be used to simulate the diffractions from complicated diffracting geometries. This method solves the problems in the frequency domain and often meets difficulties at and near shadow and reflection boundaries. Based on Huygen's principle, the Kirchhoff diffraction method (e.g. Trory, 1970; Berryhill, 1977) directly solves problems in the time domain. Because this method is supported by wave theory it can avoid the difficulties of methods based on geometric theory.

In this paper, the Kirchhoff diffraction method is used to produce synthetics for comparison with the physical modeling data.

THE MODEL AND DATA

The physical model was made of acrylics and its volume is $5700 \times 3550 \times 500$ mm^3. The velocity of the material is 2750 m/s . Grooves were cut at the bottom with the widths increasing from 1 mm to 10 mm. The height of the grooves is 5mm (figure 1). The zero-offset survey was taken at the middle of the top along a line perpendicular to the grooves.

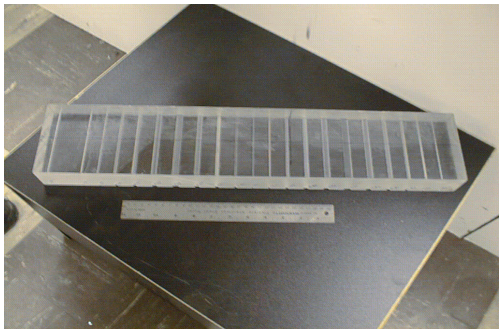

Figure 1. Photograph of the physical model.

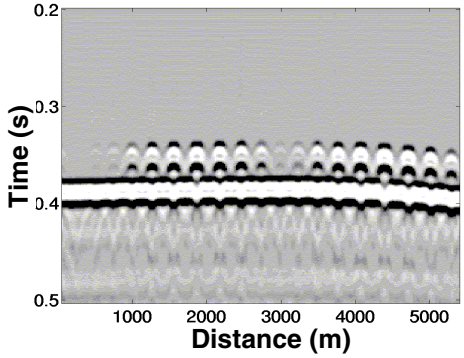

Figure 2. The physical modeling data.

Using a scaling factor of 1:10,000 for distance and time, and unity for velocity, Figure 2 shows the physical modeling data with trace interval of 20 m (scaled) and recording time interval of 0.001 second (scaled). The data contain two main features: one is the reflection from the flat top between the groves and the bottom of the model, and the other is diffractions from the edges of grooves. The diffractions in the data blur the resolution of individual groves.

THE CHARACTERISTICS OF KIRCHHOFF DIFFRACTION METHOD

Based on the Kirchhoff approach, the solution to the acoustic wave equation for zero-offset can be written as (Hilterman, 1970)

$$p(t) = \frac{1}{2\pi}\int[\frac{1}{r}f(t-\frac{2r}{c}) + \frac{1}{c}\frac{\partial}{\partial t}f(t-\frac{2r}{c})]\frac{\cos\theta}{r^2}dA \tag{1}$$

where c represents the velocity , f a source wavelet, θ is the angle between the normal to the surface $\hat{n}$ and the direction of receiver location, r is the distance from a point on the integral surface to the receiver and dA is integral element (Figure 3).

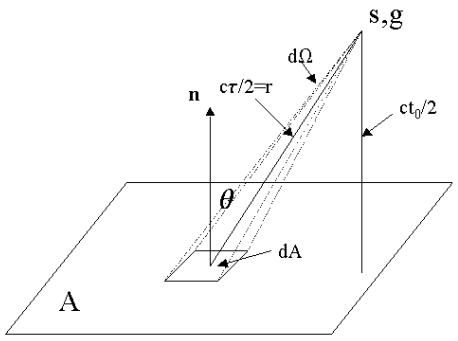

Figure 3. Geometry for the integral in the Kirchhoff diffraction method.

It is observed that $\frac{\cos\theta}{r}dA = d\Omega$, i.e. the differential element of solid angle. The angle Ω is a valid function of τ, $\tau = 2r/c$ the two-way traveltime, defined to be zero until some time $\tau = \tau_0$ at which the expanding wavefront first contacts A, and increasing monotonically thereafter. Therefore, the variables in equation (1) may be changed to be

$$p(t) = \frac{1}{2\pi c}\int [\frac{2}{\tau} f(t-\tau) + \frac{df(t-\tau)}{dt}]\frac{d\Omega}{d\tau} d\tau \tag{2}$$

By comparing the definition of a convolution

$$f(t) * g(t) = \int f(t-\tau) g(\tau) d\tau \,, \tag{3}$$

equation (2) can be written as

$$p(t) = \frac{1}{2\pi c}[f(t) * \frac{2}{t}\frac{d\Omega}{d\tau} + \frac{df(t)}{dt} * \frac{d\Omega}{d\tau}] \tag{4}$$

Using the relation $\frac{df(t)}{dt} * g(t) = f(t) * \frac{dg(t)}{dt}$, then we have (Berryhill, 1977)

$$p(t) = f(t) * D(t) U(t - t_0) \tag{5}$$

where U denotes the step function and $D(t)$ the normalized diffraction response dependant upon the geometry of observation. Equation (1) shows that a diffraction can be expressed as the result of a wavelet convolved with a diffraction response. Therefore, the key to this method is to find the diffraction response $D(t)$, which depends upon the particular problem.

For the zero-offset case, the diffraction response operator, D, due to the termination of a planer reflector can be calculated via

$$D(t') = \frac{\cos\theta_0}{\pi} \frac{t_0^2}{(t'+t_0)^2} \frac{d}{dt'} [\arctan(\sqrt{t'(t'+2t_0)}\,/(t_0 \sin\theta_0))] \tag{6}$$

where $t'=t-t_0$ is time measured after the onset time t_0 , θ_0 is the angle between the normal to the reflecting plane and ray path of the minimum travel time (Figure 3). This operator alters the intrinsic shape of the wavelet, in addition to changing its overall amplitudes. Calculation of D requires knowledge of only two parameters, i.e. t_0 and θ. In practical applications, D is evaluated numerically with t' taking values that are multiples of a discrete time sample interval. The details of the derivation and analysis of equation (6) can be found in Berryhill's paper (1977). Here, only the main properties of the pulse responses for zero-offset seismic experiments are outlined as follows:

a) Diffraction amplitudes are frequency dependent: high frequency pulses excite less diffraction response than that of low frequency pulses, and the waveform changes shape along a diffraction hyperbola because high frequency components die out first.

b) The maximum amplitude that a diffraction can attain is one half that of the associated reflection. Maximum amplitude occurs where the diffraction meets the reflection.

c) Diffraction hyperbolae are divided into two regions in which the algebraic signs of the amplitudes are opposed. The part of the hyperbola away from the associated reflection has the same polarity as the reflection, while the part beneath the reflection (if visible) has the opposite polarity.

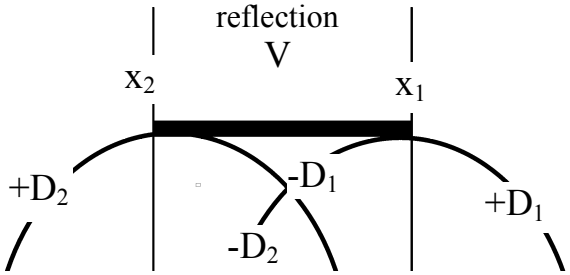

Figure 4. Response from plane strip. Strip is parallel to *y* axis with edges distant x_1 and x_2 from the normal through source-receiver.

Equation (6) is for the calculation of diffraction from a single edge. It can also be applied to more complicated *2D* geometries with plane strips approximation. For each plane strip the response operator can be written as

$$D_s(t) = V + D_2 + D_1 \tag{7}$$

where D_1 and D_2 are the responses from the edges at x coordinates equal to x_1 and x_2, respectively (Figure 4), and V is the reflection from the reflector between x_1 and x_2. Clearly, if $x_1=x_2$ the response is zero as it must be expected for a reflection from a zero surface area. Figure 5 presents the seismic response calculated for four short reflector segments. Each pattern is the sum of a reflection and two diffractions. This figure addresses the question of how small a reflector can be distinguished by the seismic method and may provide additional information about diffraction for seismic data interpretation.

SIMULATING RESULTS

In practical applications of equation (5), D is evaluated numerically with t' taking on values which are multiples of some discrete time sample interval. When θ_0 is zero degrees, D is a one sample spike whose magnitude should be exactly one-half. However, numerical evaluations for $\theta_0=0$ may be difficult because of the singularity at this point in equation (2). In stead of evaluating $\theta_0=0$, a small angle can be used as an approximation.

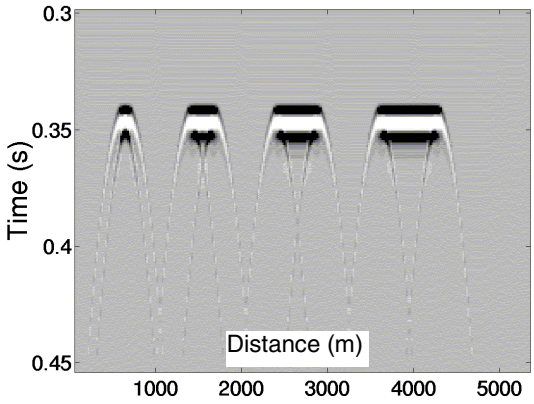

Figure 5. Combined reflection and diffraction response for four reflectors of varied lateral extent.

In order to apply equation (7), the model was further simplified (Figure 6), where the reflectors were composed of a discontinuous reflector that models the bottom of the model and small reflectors that model the top of groves. Because of the zero-offset experiment the effects from the sides of groves are neglected. With this simplified model, equation (7) can be applied to each segment as a finite strip case and then the total responses can be obtained by summing all of responses.

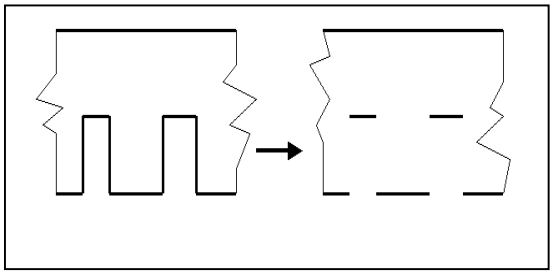

Figure 6. Schematic simplification of the model.

The source function used in the simulation is extracted directly from the recorded reflection signal from the bottom of the model (Figure 7).

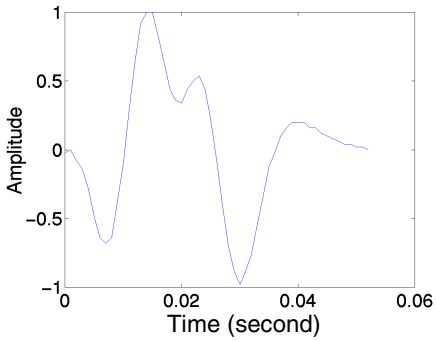

Figure 7. The source function used in the simulation.

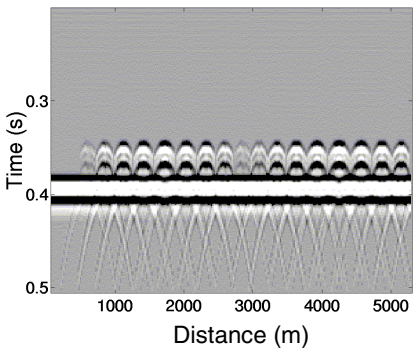

Figure 8. The simulated result.

Assuming that both source and receiver signal have finite dimensions rather than a point source, the averages of the results from four neighboring point sources and receivers are used as the final simulated data. The simulated result is shown in figure 8, which is roughly comparable to the acquired physical modeling data. Comparing this result with the measured data (Figures 9 and 10), except for some details they match quite well.

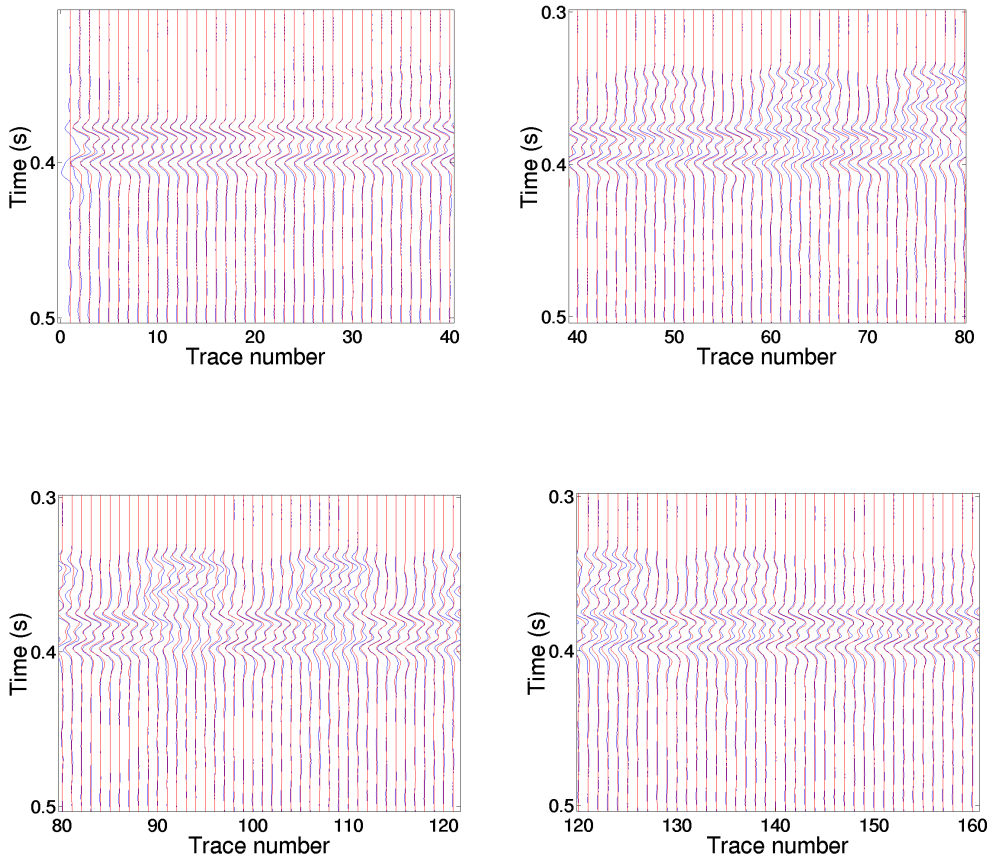

Figure 9. The comparisons between the physical modeling data and simulated data.

DISCUSSIONS AND CONCLUSIONS

The Kirchhoff diffraction method was used for the simulation of physical modeling data. This method has a simple formulation and gives an understandable physical explanation of Huygen's principle. The result of simulation shows that the Kirchhoff diffraction method can approximately predict the physical model measurement and therefore, it can be used for further investigation of the effects of diffractions.

The results show that the simulated data does not perfectly fit the measured data. This may come from the far-field approximation in the theory and the model used in the simulation may be over simplified. In the method, the source function is assumed to be isotropic. However, the real source function may be directionally anisotropic,

which may also lead to misfit between the simulated data and the physical modeling data.

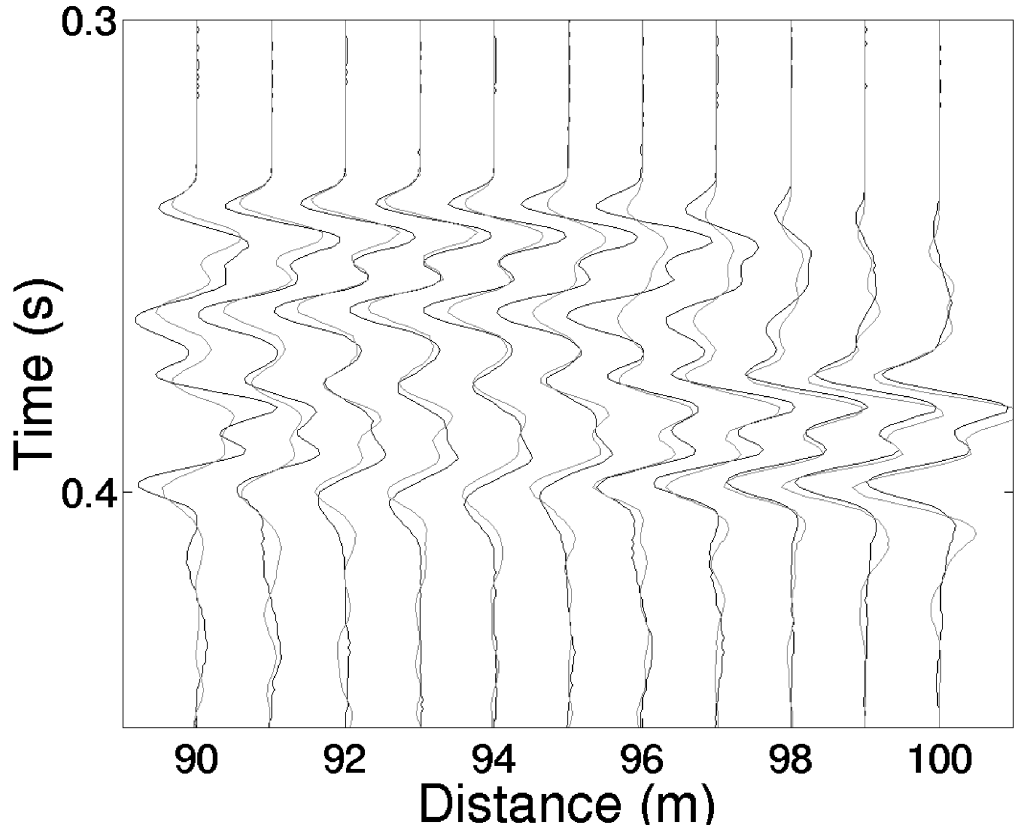

Figure 10. The comparisons between the physical modeling data (black) and simulated data (gray).

ACKNOWLEDGEMENT

We thank the sponsors of the CREWES Project for their financial support.

REFERENCES

Trorey, A.W., 1970, A simple theory for seismic diffractions: Geophysics, **35**, 762-784.

Berryhill, J.R., 1977, Diffraction response for nonzero separation of source and receiver: Geophysics, **42**, 1158-1176.

Kanasewich, E.R. and Phadke, S.M, 1988, Imaging discontinuities on seismic sections: Geophysics, **53**, 334-345.

Keller, J.B., 1962, Geometrical theory of diffraction: J. Opt. Soc. Am., **52**, 116-130.

Kouyoumjian, R.G. and Pathak, P.H., 1974, A uniform geometrical theory of diffraction for an edge in a perfect conducting surface: Proc. IEEE, **62**, 1448-1461.

Zhang, Q. Jull. E.V. and Yedlin, M.J., 1990, Acoustic pulse diffraction by step discontinuities on a plane: Geophysics, **55**, 749-756.